Highlights

Sugar as a Temporary Cementing Agent for Sand: A Simple and Reversible Soil Stabilisation Technique

Gianmario Sorrentino, Andrea Franza, Irene Rocchi

- Sugar-cemented sand is proposed as a biodegradable and reversible stabilisation for dry coarse-grained soil.
- UCS exceeded: 6 MPa at 40% sugar concentration under optimal curing; 1 MPa across all testes.
- Stress–strain curves were nearly linear up to peak, followed by a softening response.
- SEM imaging confirmed sugar crystallisation at grain contacts, forming interparticle bonding structures.

Sugar as a Temporary Cementing Agent for Sand: A Simple and Reversible Soil Stabilisation Technique

Gianmario Sorrentino[a,*,1], Andrea Franza[b,2] and Irene Rocchi[c,**,3]

[a]Technical University of Denmark, Department of Environmental and Resource Engineering Geotechnics & Geology, 2800 Kgs. Lyngby, Denmark
[b]Department of Civil and Architectural Engineering - Structural Dynamics and Geotechnical Engineering, Aarhus University, Aarhus, 8000, Denmark

ARTICLE INFO

Keywords:
Sand cementation
Sugar-based stabilisation
Unconfined compressive strength (UCS)
Biodegradable soil treatment
Temporary ground improvement

ABSTRACT

This study investigates the use of sugar as a low-viscosity cementing agent for enhancing the mechanical behaviour of sand. Dry sand was mixed with aqueous sugar solutions of varying concentrations (15%–40% by mass) and oven-cured at different temperatures. Unconfined compressive strength (UCS) tests showed that strength increased with sugar concentration, with UCS values reaching up to 6 MPa —comparable to or exceeding those achieved with conventional bio-cementation methods. Optimal curing occurred at 105 °C, balancing rapid hardening and peak strength, while excessive heating at 170 °C reduced strength due to sugar caramelisation. Nevertheless, all conditions yielded mean UCS values above 1 MPa, demonstrating the method's reliability. Scanning electron microscopy (SEM) was used to observe the interaction between sugar and sand particles, revealing a substantial sugar coating bonding the grains. This research supports sugar-based cementation as a non-toxic and biodegradable ground improvement technique for coarse-grained soils in dry conditions, particularly suited for short-term applications.

1. Introduction

The stabilisation and cementation of sandy soils represent a critical area of geotechnical engineering, with wide-ranging implications for construction, environmental protection, and disaster mitigation (Makusa, 2012). Due to their loose structure and poor cohesion, sandy soils are particularly vulnerable to erosion, liquefaction, and shear instability, posing challenges for infrastructure development and resilience in many regions (Mitchell and Soga, 2005; Huang and Hartemink, 2020). Historically, various techniques have been employed to improve the mechanical properties of sandy soils (Izadi et al., 2022; Khatami and O'Kelly, 2013; Tester, 1990; Prabakar et al., 2004; Haeri et al., 2000; Edinçliler et al., 2010). Traditional approaches include mechanical compaction and densification through methods like vibroflotation, which enhance soil strength but can cause significant environmental disturbance. Chemical grouting emerged as an alternative, offering greater control and improved performance (Kazemian et al., 2010). However, the introduction of synthetic chemicals has raised concerns regarding environmental contamination, toxicity, and long-term sustainability (Jefferis, 2003).

In recent years, bioengineering techniques have gained attention as more sustainable and eco-friendly solutions. Among these, Microbial Induced Calcite Precipitation (MICP) has emerged as a leading method. MICP employs microorganisms—typically ureolytic bacteria—that produce urease, an enzyme that catalyzes the hydrolysis of urea into ammonium and carbonate ions (Konstantinou et al., 2021; Jiang and Soga, 2017). In the presence of calcium, these carbonate ions form calcium carbonate (calcite), which precipitates within the soil matrix. This process binds soil particles together, mimicking natural cementation and significantly improving soil strength and stiffness. MICP offers notable advantages: it uses naturally occurring bacteria, operates under relatively mild conditions, and produces durable calcite bonds. Its low-viscosity treatment solutions allow for better penetration and uniform distribution, making it especially appealing for complex or sensitive environments. However, despite its promise, MICP has shortcomings.

*Corresponding author
**Currently on leave and has not yet reviewed the final version of the manuscript. Authorship will be confirmed before journal submission.
giaso@dtu.dk (G. Sorrentino); anfr@cae.au.dk (A. Franza); ireroc@dtu.dk (I. Rocchi)
https://orbit.dtu.dk/en/persons/gianmario-sorrentino (G. Sorrentino);
https://pure.au.dk/portal/en/persons/anfr$%$40cae.au.dk (A. Franza);
https://www.dtu.dk/english/person/irene-rocchi?id=116103&entity=profile (I. Rocchi)
ORCID(s): 0000-0002-9890-6032 (G. Sorrentino); 0000-0001-7109-708X (A. Franza)

One major concern is the production of ammonia as a byproduct of urea hydrolysis (Zhelezova et al., 2025). Ammonia release poses environmental and health risks (Ryer-Powder, 1991), especially when applied at scale, and this issue is often underrepresented in discussions about MICP's sustainability (Zhelezova et al., 2025).

This study explores sugar as an innovative binder for temporary sand cementation. While the idea may seem unconventional, it is not entirely without precedent. Sugar was first used by Mould (1983) to artificially cement sand cubes for testing purposes in his doctoral work on stress-induced anisotropy (Mould, 1983); later, Sture et al. (1999) employed sugar-cemented sand specimens to investigate fracture and size effects in cemented geomaterials (Sture et al., 1999). Despite these previous works, sugar has been used primarily as a means to prepare specimens for mechanical testing of pseudo-rock materials, and little emphasis was placed on the degree of cementation itself and its mechanisms. Importantly, neither study systematically evaluated the mechanical performance of sugar-cemented sand using standard geotechnical protocols, such as unconfined compressive strength (UCS) testing, and the interlinked effects of curing procedure and sugar concentrations on strength and stiffness properties of sugar-cemented sands. Characterising the correlation between sugar contents and curing methodology to geotechnical mechanical parameters is relevant to enable engineering applications in which biodegradable or non-permanent stabilisation is desired: for instance, temporary ground improvements in arid areas (Abdelhak, 2022; Nemati, 1986), erosion control in environmentally sensitive areas (Kosmas et al., 2006; Imani et al., 2025), or time-sensitive scenarios such as rapid preparation of temporary airstrips or access routes in emergency or military contexts (Rafalko, 2006; Petersen et al., 2025).

This paper investigates the extent to which sugar solutions can improve the strength and stiffness of sand under dry conditions. First, the mechanical response of sugar-treated sand is characterised through displacement-controlled UCS testing, in addition to a microstructural analysis of sugar-grain bonding. Finally, the cementing effect is expected to be reversible upon exposure to water, owing to the inherent solubility of sugar. Our goal is not to propose sugar as a replacement for microbial-induced calcite precipitation (MICP) or conventional stabilisers, but to highlight a simple, low-toxicity, and potentially reversible mechanism for temporary soil improvement.

2. Theory of the proposed concept and research hypothesis

2.1. Background on sugar cake formation

The tendency of sugar particles (sucrose, $C_{12}H_{22}O_{11}$) to form solid masses or "cakes" under varying humidity conditions is a well-documented phenomenon in the literature (Meadows, 1993; Leaper et al., 2003; Sorrentino, 2022). This process, commonly referred to as "caking", occurs when sugar crystals interact under conditions of high relative humidity, leading to interparticle bonding and a loss of free-flowing behaviour. According to Meadows (1993), each sugar particle typically consists of a central core of inherent moisture, surrounded by a layer of bound water. As environmental humidity increases, these outer moisture layers become mobile, allowing adjacent sugar particles in contact to form a liquid bridge—a pendular bridge—due to surface dissolution and recrystallization. At the points of contact, surface crystallization occurs, effectively "gluing" the particles together through intercrystalline bridging. This mechanism is central to the undesired clumping of sugar in storage environments.

In this study, we explore how this same mechanism can be repurposed as a beneficial process for sand stabilisation. When sugar is added to water, it undergoes dissolution—a physical process that disrupts its highly ordered crystalline structure (Atkins et al., 2005; Pérez, 1995). In the solid phase, sugar molecules are held together by a dense network of hydrogen bonds, giving sugar its rigidity and granular appearance (Pérez, 1995). Upon contact with water, the polar water molecules interact with the hydroxyl groups (-OH) on the sucrose, gradually breaking the intermolecular bonds that maintain the crystal lattice. This endothermic process leads to the hydration of individual sucrose molecules, effectively dispersing them into the solution. At this stage, sugar exists not as a visible particle, but as freely moving hydrated molecules in dynamic equilibrium within the solvent. As water evaporates from a sugar solution, sugar molecules begin to recrystallize. The resulting crystalline bridges can generate measurable cohesion; for example, Leaper et al. (2003) reported compressive strengths of recrystallized sugar structures up to 150 Pa, highlighting the potential of solidified sugar to act as a binding phase.

2.2. Concept and Mechanisms of Sugar-Based Sand Cementation

When applied to sand, the sugar-cake formation process can be harnessed as a binding mechanism: as water evaporates, sugar bridges form between adjacent sand grains, effectively producing a hardened structure. Fig. 1 illustrates the underlying mechanism of sugar-based sand cementation: (i) the sand matrix is initially (nearly) saturated with an aqueous sugar solution, which partially fills the pore spaces between particles; (ii) during drying, the sugar

solution migrates toward intergranular contact zones as evaporation progresses due to capillary forces; (iii) as the water content further decreases, dissolved sugar recrystallises near contact points, forming solid bridges that cement adjacent grains into a bounded structure. Unlike traditional cementitious binders that rely on chemical hydration reactions, sugar-induced cementation is a physical process governed by crystallisation and hydrogen bonding between sugar molecules and the sand grain surfaces—particularly at grain contact points.

This mechanism is reversible and potentially biodegradable—key advantages for temporary or environmentally sensitive ground improvement. In contrast to traditional binders, sugar-based cementation relies on physical crystallisation rather than irreversible chemical reactions, allowing the bonds to be dissolved upon rewetting. This property is particularly beneficial in applications requiring temporary stability, such as short-term construction, erosion control, artistic installations, or biodegradable structures. However, the system is highly sensitive to moisture, which poses a significant limitation for long-term or permanent use.

Another practical advantage is that, at the concentrations of interest, the viscosity of sugar solutions remains close to that of pure water. Aqueous sugar solutions exhibit an approximately linear increase in viscosity with sugar concentration (Kim, 2010); for instance, while pure water has a viscosity of 0.001 Pa s, a 20% sugar solution reaches about 0.0012 Pa s. This modest increase does not significantly affect the hydraulic conductivity of the sand, as meaningful changes in permeability typically require at least a tenfold increase in fluid viscosity. This low viscosity of sugar solutions presents a practical advantage: it enables the binding solution to infiltrate the pore space of the granular matrix without disturbing the soil's inherent porosity or structure (Zhu et al., 2024). As a result, effective and uniform cementation can be achieved throughout the specimen, supporting applications in porous media where consistent penetration is critical.

Building on previous findings and the known physicochemical behaviour of sugar during dissolution and recrystallisation, this study tests the hypothesis that sugar-cemented sand can attain stiffness and strength levels comparable to pseudo-rock materials. Specifically, we expect performance within the same order of magnitude as sands stabilised via MICP. To test this hypothesis, we conducted unconfined compressive strength (UCS) tests under varying preparation and curing conditions, complemented by Scanning Electron Microscopy (SEM) analysis of sugar-recrystallised structures at grain contacts. These insights lay the groundwork for optimising sugar as a novel, low-impact soil stabiliser.

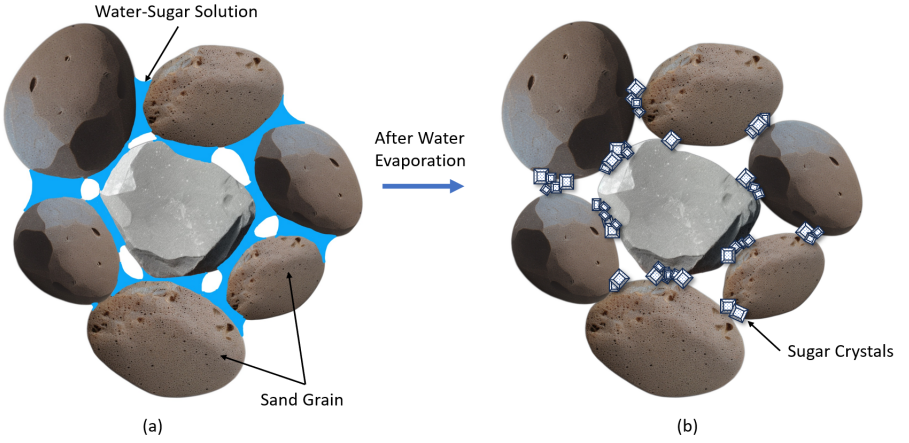

Figure 1: Visualization of sugar-based cementation in sand: (a) Sand partially saturated with an aqueous sugar solution, showing liquid occupying pore spaces; (b) Same sand sample after drying, with sugar crystals formed between grains, acting as cementing bridges that bond the particles together.

3. Materials and Methods

3.1. Materials

The soil used in this study is a silica sand supplied by Dansand. This is a poorly graded sand with median diameter d_{50}=0.36 mm, a uniformity coefficient $U = 2.10$, and curvature coefficient $C_f < 1$ (Das, 2019; ASTM, 2017). Tab. 1 summarises its physical and chemical properties. Fig. 2a displays a microscope image of this sand, while Figs. 2b

and 2c show the particle shape visualizations and particle size distribution, respectively, obtained using the QICPIC dynamic image analyser at the National Research Facility for Infrastructure Sensing (NRFIS) of the University of Cambridge (UK). This technique captures high-resolution binary black-and-white images of particles in motion (Fig. 2b), from which shape descriptors are extracted. The analysis included over 27 500 particles, ensuring statistically robust characterization of both size and shape distributions. For particle sizing, the Equivalent Projected Circle (EQPC) diameter was used—defined as the diameter of a circle with the same projection area as the particle. The QICPIC-based particle size distribution aligns well with supplier data, see Fig. 2c. The sugar used in this study was standard household granulated sugar.

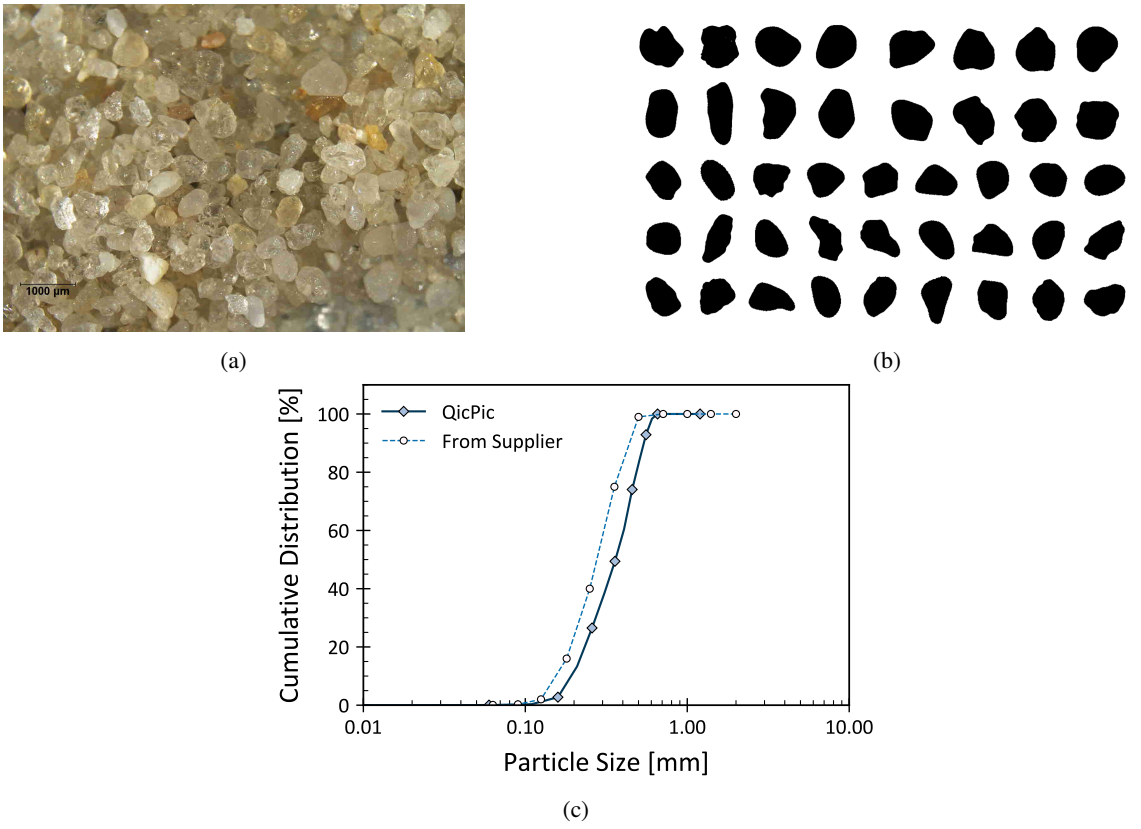

Figure 2: Silica sand used in this study. (a) Optical microscope image of the sand; (b) binary image showing particle morphology obtained from QICPIC analysis; (c) particle size distributions obtained from supplier data and QICPIC image-based measurement.

3.2. Sample Preparation

Standardised cylindrical specimens for unconfined compressive strength testing were prepared in accordance with established procedures (ASTM, 2010). Open-ended steel moulds (EN 10305), fabricated by cutting standard steel piping, were used for specimen preparation. Each mould had an internal diameter of 40 mm and a height of 85 mm. The use of open-ended moulds was a cost-effective solution; however, the absence of end-sealing allowed some moisture loss, which could not be precisely quantified during preparation but was considered negligible for the purposes of this study. Specimens were prepared in a partially saturated state to ensure consistent moisture control throughout mixing and curing. The preparation steps are illustrated in Fig. 3 and detailed below:

- *Steps 1 and 2:* Sugar was first added to distilled water and mechanically stirred using a stirrer to create sugar solutions of varying concentrations—specifically 15%, 20%, and 40% by mass, relative to the total solution mass.
- *Steps 3 and 4:* The sugar solutions were thoroughly mixed with dry silica sand in a stainless-steel mixing bowl using a hand-held spatula until a homogeneous mixture was achieved. For all specimens, the amount of sand

Table 1
Summary of physical and chemical properties of the tested sand.

Property	Value	Unit	Description
Shape Descriptors			
Sphericity	0.82 (±0.037)	–	
Aspect Ratio	0.72 (±0.117)	–	
Convexity	0.96 (±0.016)	–	
Roundness	0.34 (±0.110)	–	
Particle Size Distribution			
D10	0.19	mm	Diameter at 10% passing
D30	0.27	mm	Diameter at 30% passing
D50	0.36	mm	Median diameter
D60	0.41	mm	Diameter at 60% passing
D90	0.54	mm	Diameter at 90% passing
Uniformity Coeff. (U)	2.10	–	D_{60}/D_{10}
Curvature Coeff. (C_z)	0.95	–	$D_{30}^2/(D_{10} \cdot D_{60})$
Chemical and Physical Properties			
SiO_2 content	99.08	%	Silicon dioxide content
Al_2O_3 content	0.457	%	Aluminum oxide content
Grain density	2.640	$\mathrm{g\,cm^{-3}}$	
Bulk density	1460–1610	$\mathrm{kg\,m^{-3}}$	Minimum to maximum bulk density

used was adjusted to achieve a target void ratio, $e = 0.79$ (corresponding to a relative density $D_r = 15\%$), while the sugar solution was added to reach a water content of 25% by mass of dry sand, resulting in a degree of saturation $S_r \approx 85\%$.

- *Step 5:* Specimens were prepared using the moist tamping (MT) method in three compacted layers, each approximately 28 mm thick (one third of the total specimen height), following the procedure described by Chen and Yang (2023). A sheet of baking paper was placed around the mould to reduce friction and facilitate clean extraction. The moist sand was weighed and carefully deposited into the mould. Each layer was compacted using a metal tamper to achieve uniform height and density. The interfaces between layers were lightly scratched to improve bonding. This preparation method ensures consistent specimen quality by maintaining uniform saturation along the specimen height and by minimising segregation, particularly for sand–fines mixtures.

- *Step 6:* The specimens were oven-dried at controlled temperatures to constant mass (effectively 0% relative humidity) using three different curing protocols (referred to as CT60, CT105, CT170), to investigate the influence of temperature on hardening behaviour, as listed below. All specimens remained in the mould during curing.

  - *CT60*, drying at 60 °C for approximately four days, as shorter durations were found insufficient based on physical assessment of the sample's hardness.
  - *CT105* drying at 105 °C for 24 hours, although specimens visibly hardened earlier. The 24-hour duration was maintained across all CT105 samples to ensure consistency.
  - *CT170* drying at 170 °C for up to 5 hours. Signs of smoke were observed beyond this time, so the duration was limited to prevent sugar burning.

  After drying, the dry density was measured and found to be approximately $1.55\,\mathrm{g\,cm^{-3}}$, with low variability ($\pm 0.02\,\mathrm{g\,cm^{-3}}$). This consistency confirms the effectiveness of the moist tamping method in producing uniformly compacted specimens.

- *Step 7:* Once dried and hardened, the specimens were extracted from the moulds using a hydraulic piston. Only intact samples were retained for UCS testing, while damaged specimens were discarded. Accepted samples were stored at ambient laboratory temperature prior to testing.

Figure 3: Steps of the sample preparation.

3.3. Mechanical Testing

Unconfined compressive strength tests were performed on sugar-cemented samples using a displacement-controlled loading frame (Instron), available at the DTU Construct laboratory. The tests were conducted by applying a constant vertical strain rate while recording the mobilised axial resistance, enabling the capture of both peak strength and post-peak softening behaviour. This simple and replicable testing configuration is widely used to assess the performance of bio- and chemical-cementation methods (Abbasi et al., 2025; Rahman et al., 2020), and was selected to facilitate direct comparison with literature data and support future research.

The procedure followed standard guidelines (ASTM, 2010), with each specimen having a height-to-diameter ratio (H/D) greater than 2. An axial displacement rate of 0.7 mm min^{-1} was imposed, corresponding to an axial strain rate within the recommended range of 0.5 % min^{-1} to 2 % min^{-1}. Throughout the tests, axial force and vertical displacement were continuously recorded. These measurements were used to compute axial stress and strain, and to derive key mechanical parameters, including the unconfined compressive strength (UCS), the secant modulus at peak stress ($E_{sec,UCS}$), and the secant modulus at 50% of UCS ($E_{sec,50}$). For the sake of clarity, in this work, the UCS value was determined as the peak axial stress, identified directly from the experimental stress–strain response at the maximum of the curve as described in ASTM (2010).

4. Results of Unconfined compressive strength testing

Tests are labelled in terms of sugar concentration (15%, 20%, and 40%, respectively labelled SC15, SC20, SC40) and curing temperatures (60 °C, 105 °C and 170 °C labelled, respectively, CT60, CT105, CT170), while T# indicates the test number: e.g. SC20-CT170-T2 is the test number 2 for 20% sugar and curing temperature of 170 °C.

Tab. 2 summarises the entire unconfined compressive strength experimental campaign, including tested configurations and key mechanical results. For each combination of curing protocol and sugar concentration, Tab. 2 reports mean values of main mechanical parameters (peak resistance UCS, along with secant stiffness at peak $E_{sec,UCS}$ and at 50% peak resistance $E_{sec,50}$). In addition, selected correlations between mean UCS values, sugar concentration, and curing temperature are plotted in Figs. 4 and 5, along with standard deviations.

First, the level of variability in results in Tab. 2 is addressed. The UCS values are characterised by a relatively low coefficient of variance (CV) with ranges between 7%–16%, between samples with similar preparations; thus, UCS is a suitable parameter to characterise the mechanical behaviour, with mean values that spanned 1–6 MPa: as later discussed, there is a strong correlation betweeen UCS, sugar content, and curing procedure. Contrarily, there is a greater variability in the coefficient of variance of the secant stiffness values E_{UCS} and E_{50} that ranges between 20% and 60%. Mean secant stiffness values have a weak correlation with sugar content in samples curing with ideal conditions CT105, giving mean $E_{UCS} \approx 300$ MPa. On the other hand, there is some correlation between curing procedure and stiffness, given that both CT60 and CT170 gave lower mean $E_{UCS} \approx 150$ MPa. Therefore, it is not suggested to correlate stiffness to UCS values, and measured secant stiffness values should not be considered representative for design, given

Table 2
Summary of unconfined compressive strength (UCS) test results

Test	Sugar Concentration [%]	Curing Temperature [°C]	UCS [MPa]	ϵ_{UCS} [-]	$E_{sec,50}$ [MPa]	$E_{sec,UCS}$ [MPa]
SC15-CT105-T1	15	105	1.34	0.0048	283.06	281.54
SC15-CT105-T2	15	105	1.38	0.0053	286.62	258.73
SC15-CT105-T3	15	105	1.46	0.0063	293.21	230.63
SC15-CT105-T4	15	105	1.53	0.0055	192.20	277.32
SC15-CT105-T5	15	105	1.61	0.0043	220.79	373.33
SC15-CT105-T6	15	105	1.48	0.0041	209.43	363.27
mean			1.47	0.0051	247.55	297.47
std			0.10	0.0008	44.96	57.86
CV			0.07	0.17	0.18	0.19
SC20-CT105-T1	20	105	2.37	0.0072	392.87	329.82
SC20-CT105-T2	20	105	2.24	0.0045	476.58	495.97
SC20-CT105-T3	20	105	1.60	0.0141	152.82	113.39
SC20-CT105-T4	20	105	1.84	0.0080	251.39	230.40
SC20-CT105-T5	20	105	2.33	0.0097	181.14	240.56
mean			2.08	0.0087	302.29	282.03
std			0.34	0.0036	130.07	142.20
CV			0.16	0.41	0.43	0.50
SC40-CT105-T1	40	105	5.91	0.0132	463.80	448.63
SC40-CT105-T2	40	105	7.13	0.0245	181.44	254.64
SC40-CT105-T3	40	105	5.53	0.0123	475.01	326.50
mean			6.35	0.0199	315.28	343.26
std			0.84	0.0080	129.76	98.08
CV			0.13	0.40	0.41	0.29
SC20-CT60-T1	20	60	1.33	0.0099	123.90	134.42
SC20-CT60-T2	20	60	1.49	0.0105	128.56	141.37
SC20-CT60-T3	20	60	1.34	0.0130	104.85	102.89
SC20-CT60-T4	20	60	1.15	0.0055	69.43	210.37
SC20-CT60-T5	20	60	1.20	0.0074	123.47	163.24
mean			1.30	0.0093	110.04	150.46
std			0.13	0.0029	24.45	39.86
CV			0.10	0.32	0.22	0.26
SC20-CT170-T1	20	170	0.94	0.0031	20.32	306.11
SC20-CT170-T2	20	170	1.37	0.0074	175.68	184.53
SC20-CT170-T3	20	170	1.30	0.0099	137.93	131.11
SC20-CT170-T4	20	170	1.40	0.0091	155.16	66.96
SC20-CT170-T5	20	170	1.04	0.0124	85.33	84.21
SC20-CT170-T6	20	170	1.11	0.0065	45.83	171.98
mean			1.19	0.0100	103.38	157.50
std			0.19	0.0062	62.67	86.40
CV			0.16	0.62	0.61	0.55

the levels of standard deviation within the dataset. Second, the role of curing is addressed. UCS results in Tab. 2 show a clear influence of curing temperature on both the mechanical strength and the time required for specimens to harden sufficiently for testing. As the curing temperature increased from 60 °C to 105 °C, both the UCS and the hardening rate improved. For instance, samples cured at 60 °C required approximately 4 days to reach a mean UCS of 1.30 MPa, while those cured at 105 °C hardened in just 24 hours and reached a higher mean UCS of 2.08 MPa. This indicates that moderate heating promotes faster crystallisation and stronger bonding between sugar and sand particles.

Key results from UCS testing are shown in Fig. 4 that presents peak resistance from samples SC#-CT105 prepared with different sugar concentrations in the binding solution — specifically 15%, 20%, and 40% by mass. Under optimal curing (drying) conditions, there is a clear and substantial increase in unconfined compressive strength (UCS) with increasing sugar concentration, also confirmed when accounting for uncertainties in terms of standard deviation ± mean

values. In particular, tests with the CT105 curing regime have an average UCS increased from just under 1.5 MPa at 15% sugar concentration to approximately 6 MPa at 40%, indicating a fourfold enhancement in strength. Thus, sugar concentration played a critical role in strengthening the cementation bonds between sand grains under optimal curing.

Fig. 5 illustrates the impact of different curing techniques on the UCS of sample SC20-CT#. Interestingly, specimens CT170 (cured at 170 °C for 5 h) exhibited a lower mean UCS of 1.19 MPa, compared to 1.50 MPa for samples CT60 and to 2.08 MPa for CT105. This reduction in strength suggests a degradation of the bonding mechanism at temperatures of 170 °C, related to the dependency of sugar chemistry on temperature. Moderate curing temperatures (e.g., 60 °C) promote recrystallisation of dissolved sugar, enhancing intergranular mechanical interlocking and hydrogen bonding. However, excessive heating (e.g., 170 °C) initiates caramelisation—a thermal decomposition process in which sucrose breaks down into glucose and fructose, and further polymerises into larger, amorphous compounds such as caramelan and caramelen (Lee et al., 2022; Schmidt et al., 2012). These caramelised products lack the crystalline structure necessary for effective bonding and are known to form brittle, disordered matrices with reduced mechanical strength.

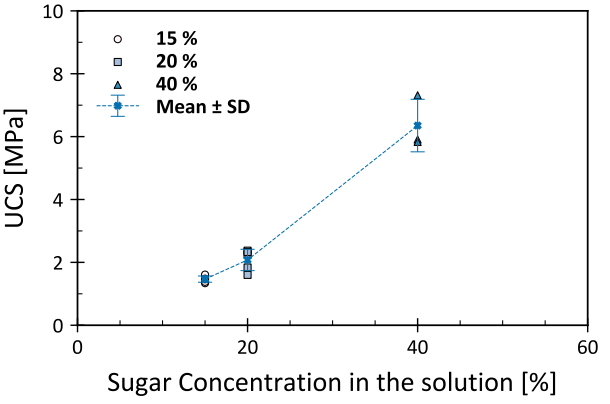

Figure 4: Relationship between sugar concentration in the suspension and UCS for tests under optimal curing (SC#-CT105). Individual markers denote experimental measurements, and error bars represent the mean UCS ± one standard deviation for each concentration level.

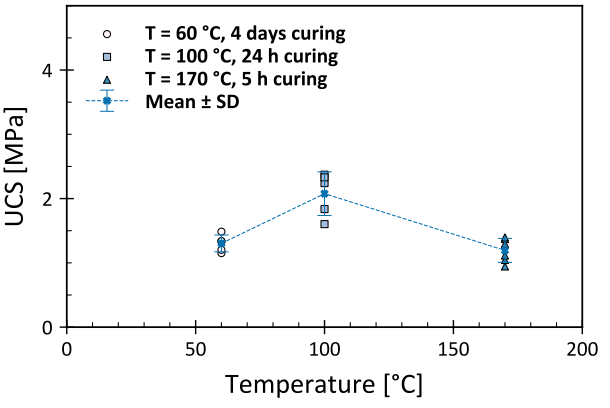

Figure 5: Relationship between curing procedure and UCS for tests at 20% sugar concentration (SC20-CT#). Individual markers denote experimental measurements, and error bars represent the mean UCS ± one standard deviation for each concentration level.

Visual inspection of the specimens after unconfined compression testing revealed a consistent failure mode across all preparation conditions, as illustrated in the selected cases shown in Fig. 6. In all cases, a distinct vertical crack developed along the axis of loading, indicative of a tensile failure mechanism commonly observed in cemented granular materials (Collins and Sitar, 2009; Tariq and Maki, 2014). Notably, while specimens with higher sugar concentrations

exhibited well-defined axial cracking typical of tensile failure, those prepared with lower sugar content often showed additional signs of localised damage at the top or bottom ends—likely due to imperfect load distribution or weaker end confinement during testing. The consistent formation of axial cracking suggests that the sugar-induced bonds form a continuous cemented matrix capable of transmitting tensile and shear stresses. As a result of observed cracking, failure occurred in tension perpendicular to the direction of maximum compressive stress, rather than by shear along failure planes. For the constitutive model of a total stress modelling of sugar-cemented sand, in addition to the measured tensile strength as a cut-off value, engineers may conservatively use this tensile strength as apparent cohesion; element testing with direct shear or triaxial devices could be used to explore the apparent cohesion law.

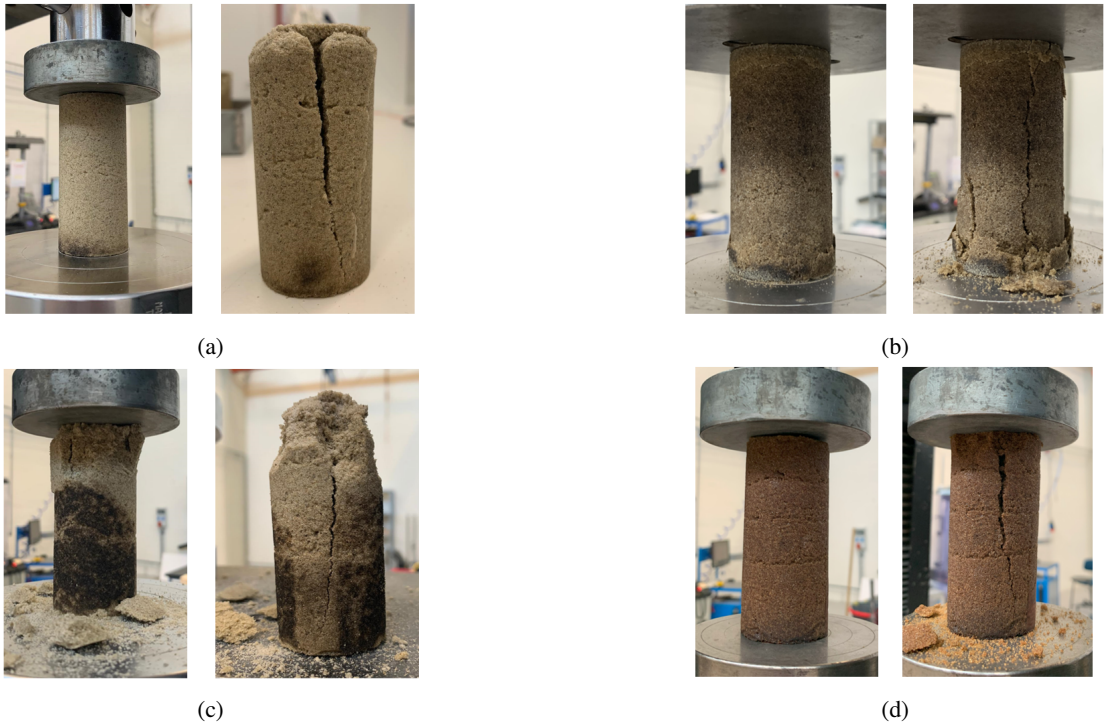

Figure 6: Photographs of UCS samples: (a) SC20-TC105-T5; (b) SC40-T105-T1; (c) SC15-T105-T1; (d) SC15-T170-T1.

To better compare failure mechanisms and material behaviour across different sample types, UCS results are graphically compared. Fig. 7 presents axial stress–strain curves from all UCS tests conducted in this study. In each row, subplots correspond to tests carried out under identical sugar concentration and temperature of curing. Fig. 7 (left-side) displays stress–strain curves as measured for fixed x-axis limits while the scale of the y-axis is adjusted, and it serves as a baseline for interpreting the mechanical response of sugar-treated sand under different conditions. Fig. 7 (right-side) shows stress-strain curves normalised by their respective UCS and strain-at-UCS ε_{UCS} values (i.e. $\varepsilon/\varepsilon_{UCS}$ vs σ/UCS), to quantify how brittle or ductile the post-peak response is compared with the shortening needed to reach peak UCS.

When analysing stress-strain in Fig. 7 (left-side), results confirmed previous observations on the interlink between sugar content, curing, and UCS, although results are characterised by localised irregular trends. In terms of slope of the stress-strain curve till peak, although data do not reveal conclusive correlations between secant stiffness E_{UCS} and sugar-cementation procedure, results indicate a concave shape at very small strains (possibly due to the sample entering in full contact with the piston) following by a nearly linear trend up to peak UCS resistance. This nearly linear mobilisation of resistance with strain is well illustrated by normalised stress-strain curves (Stress/UCS vs. Strain/ϵ_{UCS}) in Fig. 7 (right-side), particularly the averaged normalised curve reported per sub-plot.

Furthermore, for direct comparison, the averaged normalized curves from Fig. 7 (right-side) are also grouped into Fig. 8 for discussing pre-peak and post-peak trends. Normalised curves in Fig. 8a at varying concentration reveal that samples with higher sugar concentrations (e.g., SC40) exhibit a steeper post-peak drop in mobilised resistance,

associated with a high softening rate that may be described as nearly brittle. In contrast, samples with lower sugar content (SC15 and SC20) show a more gradual reduction in strength after peak, suggesting a more ductile-like post-peak response. Therefore, while increased sugar content enhances peak strength (UCS) (see Fig. 4), stress-strain curves consistently highlight that the higher the UCS from high sugar content, the less ductile is the post-peak stress-strain curve. However, it is important to note that the term "brittle" should be used with caution: although higher sugar concentrations (e.g., SC40) exhibited a sharp post-peak stress drop, all specimens retained a post-peak tail with gradual strength reduction with the strain rate. This indicates that even in the most cemented cases, failure was not perfectly brittle but showed a residual load-bearing capacity beyond the peak. In contrast, the normalized stress–strain curves for samples cured at different temperatures (and curing time) in Fig. 8b exhibit very similar shapes, indicating that while curing temperature significantly influences the peak strength (UCS), it has a limited effect on the overall deformation behaviour. This reinforces the conclusion that the mechanical response is more strongly influenced by sugar concentration than by curing temperature.

This dependence of softening rate on sugar content may relate to the number of brittle interparticle bonding per particle. In the presence of large number of cementation links, once the peak is reached, bounding break more abruptly, leaving the remaining structure less capable of redistributing load after localised bond failure. This trend aligns with established micromechanical understanding of cemented granular materials, where increased cementation typically results in more brittle stress–strain behavior. Zhang et al. (2022) showed that increasing the cement–sand ratio or curing time enhances both the number and strength of interparticle bonds, leading to higher peak and residual strengths and increased stiffness, but also sharper softening post-peak. Similarly, discrete element simulations by de Bono et al. (2015) demonstrated that increasing the number of bonds per grain shifts the failure mode from ductile to brittle, with higher UCS and reduced capacity for stress redistribution after bond breakage. The absorbed energy per unit volume was estimated by calculating the area under the stress–strain curves, using the average mechanical parameters reported in Tab. 2 and the corresponding average stress–strain trends shown in Fig. 8a. As stress and strain are normalized in the plots, the absorbed energy was obtained by integrating the normalized curves and scaling by the measured UCS values. This quantity reflects the energy required to deform and ultimately fail the sample under axial loading. The results indicate that increasing sugar concentration enhances both the unconfined compressive strength and the energy absorption capacity of the material. In particular, the SC40–CT105 configuration exhibited an absorbed energy approximately four times greater than that of SC20–CT105. This trend suggests that higher sugar content likely promotes the formation of more interparticle bonds and stronger crystallized bridges between sand grains, which improves overall stiffness, strength, and resistance to failure.

Finally, it is of interest to contextualise results with UCS values from alternative cementation techniques. The UCS values observed in this study, ranging from approximately 1.5 MPa to 6 MPa, are well aligned with—or even exceed—those typically reported for other bio- or chemically-cemented sands. For example, MICP treatments commonly produce UCS values between 1.5 MPa and 5.0 MPa, with the upper bound achieved under optimized laboratory conditions (Rahman et al., 2020; Gomez et al., 2014). Fungi-based cementation techniques, such as those utilizing Aspergillus niger, have demonstrated UCS values between 1.0 MPa and 3.9 MPa, depending on fungal strain, nutrient availability, and curing time (Fang et al., 2018; Ahmad et al., 2024). Similarly, xanthan gum biopolymers have yielded UCS values typically ranging from 0.3 MPa to 4 MPa, with strength development strongly influenced by dosage and curing conditions (Soldo and Miletić, 2019; Ding et al., 2023; Rahman et al., 2020). Therefore, compared to these established bio-cementation methods, the sugar-based cementation process explored in this study shows both higher peak strength and simpler processing requirements.

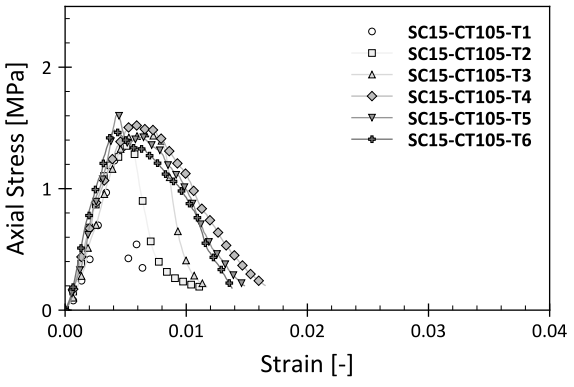
SC15-CT105-T1
SC15-CT105-T2
SC15-CT105-T3
SC15-CT105-T4
SC15-CT105-T5
SC15-CT105-T6
Axial Stress [MPa]
Strain [-]

(a)

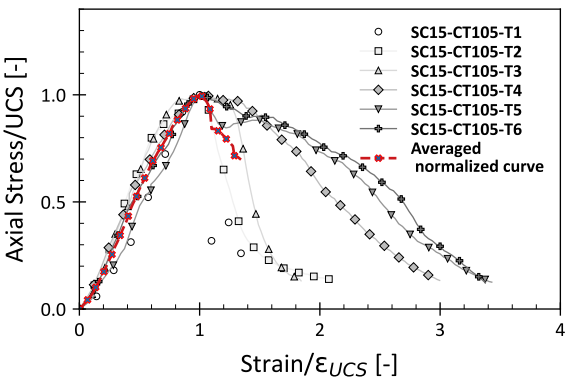
SC15-CT105-T1
SC15-CT105-T2
SC15-CT105-T3
SC15-CT105-T4
SC15-CT105-T5
SC15-CT105-T6
Averaged
normalized curve
Axial Stress/UCS [-]
Strain/εUCS [-]

(b)

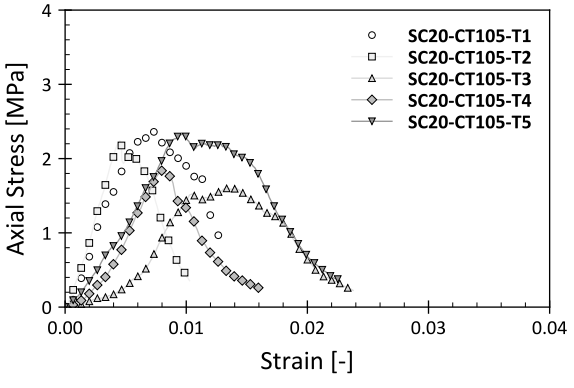
SC20-CT105-T1
SC20-CT105-T2
SC20-CT105-T3
SC20-CT105-T4
SC20-CT105-T5
Axial Stress [MPa]
Strain [-]

(c)

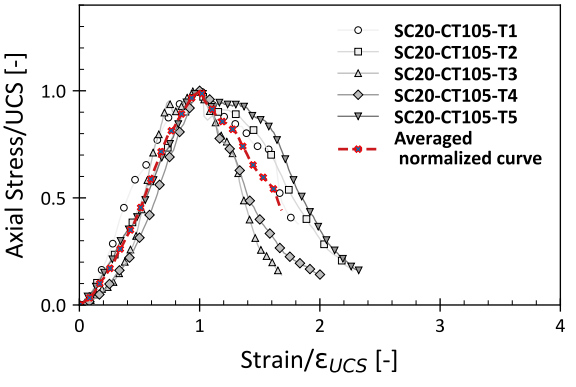
SC20-CT105-T1
SC20-CT105-T2
SC20-CT105-T3
SC20-CT105-T4
SC20-CT105-T5
Averaged
normalized curve
Axial Stress/UCS [-]
Strain/εUCS [-]

(d)

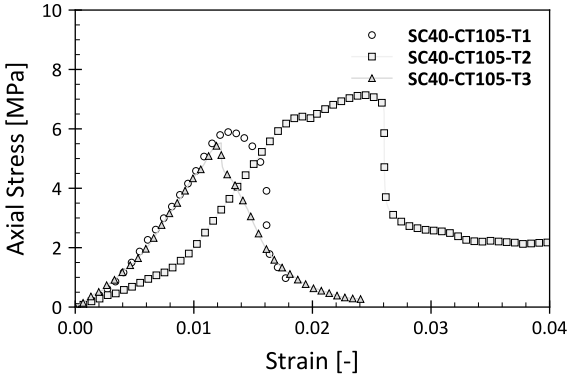
SC40-CT105-T1
SC40-CT105-T2
SC40-CT105-T3
Axial Stress [MPa]
Strain [-]

(e)

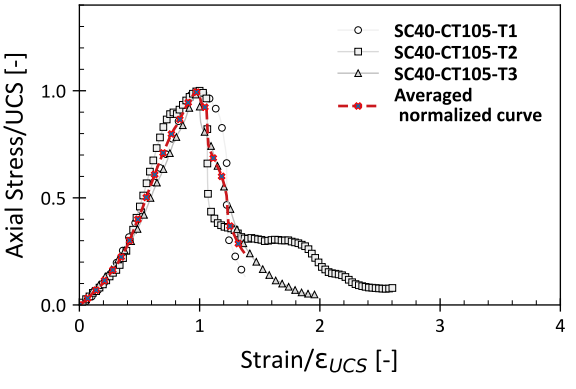
SC40-CT105-T1
SC40-CT105-T2
SC40-CT105-T3
Averaged
normalized curve
Axial Stress/UCS [-]
Strain/εUCS [-]

(f)

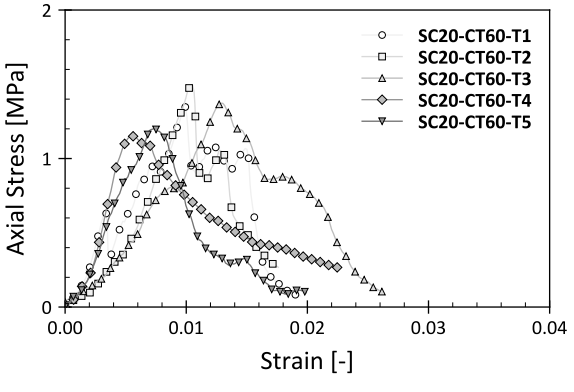
SC20-CT60-T1
SC20-CT60-T2
SC20-CT60-T3
SC20-CT60-T4
SC20-CT60-T5
Axial Stress [MPa]
Strain [-]

(g)

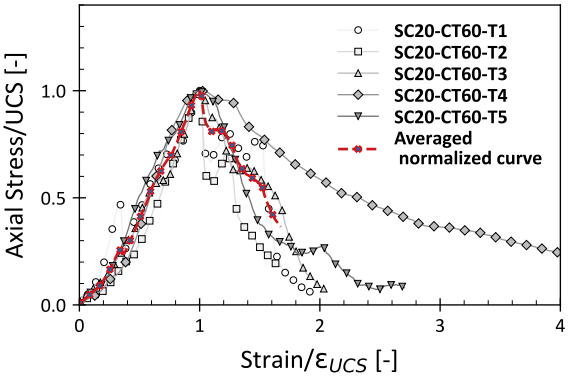
SC20-CT60-T1
SC20-CT60-T2
SC20-CT60-T3
SC20-CT60-T4
SC20-CT60-T5
Averaged
normalized curve
Axial Stress/UCS [-]
Strain/εUCS [-]

(h)

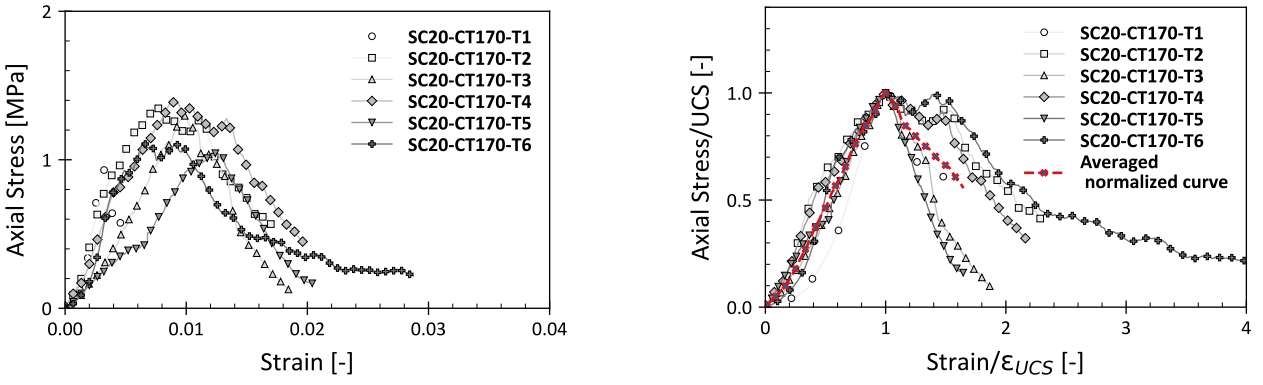

Figure 7: Unconfined compression test results showing axial stress–strain behaviour (left side) and corresponding normalized curves (right side): (a,b) 15% sugar solution, cured at 105 °C for 24 h (SC15-CT105); (c,d) 20% sugar solution, cured at 105 °C for 24 h (SC20-CT105); (e,f) 40% sugar solution, cured at 105 °C for 24 h (SC40-CT105); (g,h) 20% sugar solution, cured at 60 °C for 4 d (SC20-CT60); (i,j) 20% sugar solution, cured at 170 °C for 5 h (SC20-CT170).

5. SEM

Scanning Electron Microscopy (SEM) was employed to investigate the microstructural characteristics of the sugar-cemented sand specimens. Imaging was conducted at DTU Nanolab using the AFEG 250 Analytical Environmental SEM (ESEM), equipped with a field emission gun for high-resolution imaging and a Backscattered Electron Detector (BSED). The BSED was selected to enhance contrast based on atomic number differences, allowing for better visualization of compositional variation between sand grains and sugar crystals.

A fragment of the SC20-CT105-T5 specimen, retrieved after unconfined compression testing, was mounted on an aluminum stub using carbon adhesive tape. Although gold coating was initially applied to mitigate charging effects, clearer imaging was ultimately achieved without coating by operating the SEM under low vacuum conditions. This setup minimized charging while preserving key surface features relevant to the bonding mechanism.

As shown in Fig. 9, SEM images captured at varying magnifications reveal how sugar interacts with the sand particles. At lower magnifications (approximately ×100; Figs. 9a and 9c), sand grains appear as light grey bodies with curved edges, while sugar is distinguishable by its darker tone and angular crystalline morphology. The images also show a substantial presence of sugar surrounding the sand particles, suggesting effective distribution and coating during sample preparation, despite the 20% sugar concentration. Higher magnifications of ×1215 (Figs. 9b and 9d) provide a more detailed view of the bonding interface, showing sugar bridges that link adjacent grains. The sharp-edged crystal structure of the sugar suggests the formation of a well-defined crystalline phase. In addition, it is possible to observe how multiple grains are held together by the sugar crystals.

These sugar crystals observed in the SEM analysis certainly contributed to cementation and strength enhancement observed in the samples; further research is needed to investigate the link between micro-scale sugar crystal formations and macro-scale UPS properties.

6. Discussion on possible use

The findings of this study demonstrate that sugar-based cementation offers a rapid, simple, and biodegradable method for temporary sand stabilisation. The mechanical performance achieved, particularly mean UCS values consistently exceeding 1 MPa across all curing conditions—confirms that even short-term exposure to heated sugar solutions can lead to effective soil hardening. Peak strengths up to 7 MPa were observed for high-concentration treatments, comparable to results from more complex bio-cementation techniques.

Given its ease of application and temporary nature, this technique holds strong potential for a variety of short-term or biodegradable stabilisation needs. These include use in temporary infrastructure (e.g., unpaved roads, airstrips, or access pads), erosion control measures, or experimental geotechnical modeling where easy disaggregation or reuse of

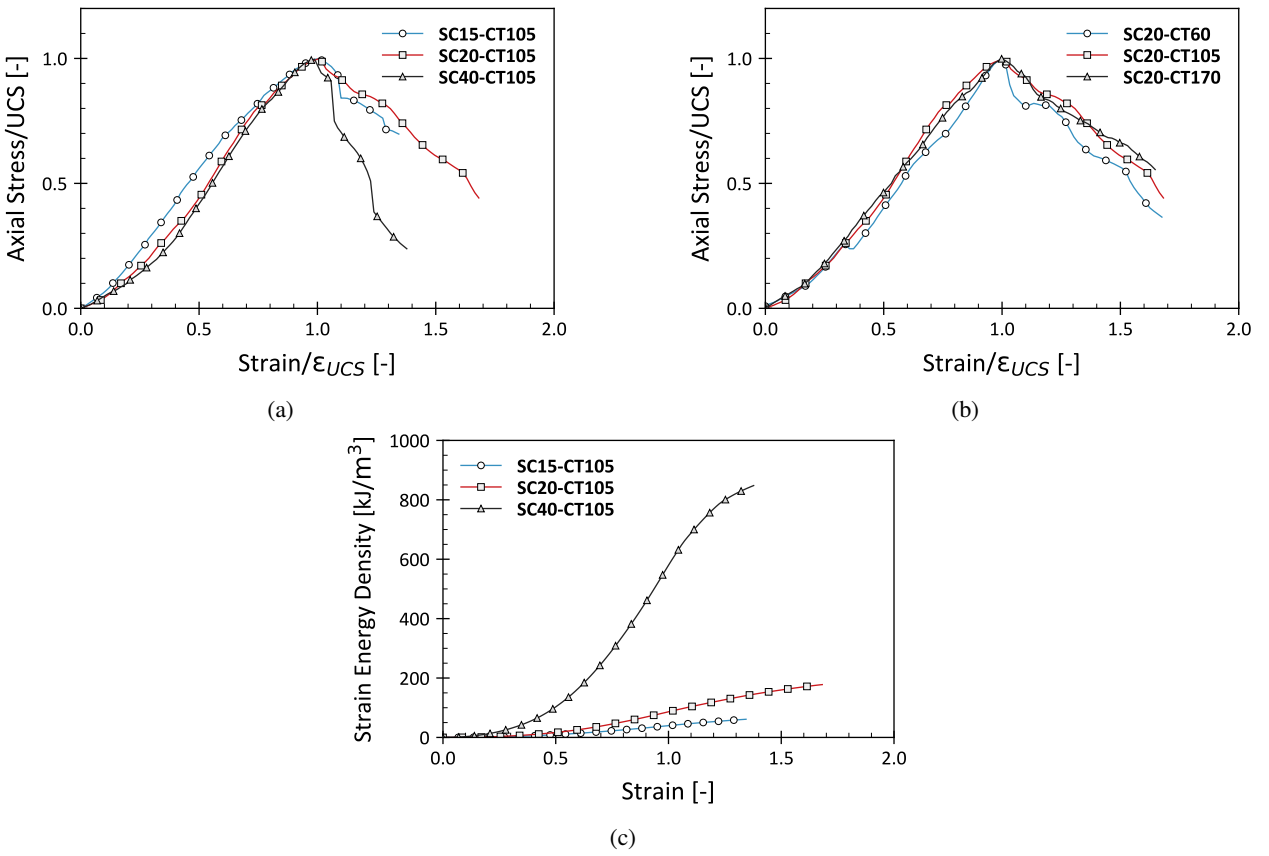

Figure 8: Mean normalized stress–strain curves (Stress/UCS vs. Strain/ϵ_{UCS}) comparing: (a) different sugar concentrations; (b) different curing; (c) Absorbed energy per unit volume.

specimens is desirable after testing. Another promising application relates to time-sensitive deployments, such as in the military, disaster relief, or construction staging environments, where a rapid but reversible ground improvement method is needed. The ability to produce immediate bonding without permanently altering the subsurface makes sugar-based cementation particularly attractive in time-constrained, non-permanent deployments.

Importantly, the use of sugar may also have longer-term ecological and bio-mediated benefits. Sugar amendments in soil are known to stimulate fungal growth and microbial activity, including enhanced phosphorus mobilization and increased presence of arbuscular mycorrhizal (AM) fungi and their associated bacteria (Jin et al., 2024). This biological response has implications for fungal-induced soil cementation, a process shown to transform loose sand into biosandstone over several days to a week. However, fungal bio-cementation requires time for colonization and mineral precipitation (Martuscelli et al., 2020; Park et al., 2025).

Therefore, the method proposed in this study could serve as a complementary solution, rapidly hardening the soil in the short term while potentially fostering fungal colonisation that supports longer-term stabilisation. This dual-phase approach could bridge the gap between immediate mechanical needs and ecologically integrated soil improvement strategies. Future work could explore this synergy with fungal colonisation with relevant aspects including: the compatibility of sugar-based hardening with fungal growth and survival; the degradation timeline of sugar bonds under variable moisture conditions; the integration with bio-stimulation strategies to transition from sugar-induced to fungus-induced cementation. Such hybrid approaches could enable adaptive soil systems that shift over time from engineered to self-sustaining bio-stabilized states, minimizing the need for external intervention while preserving performance.

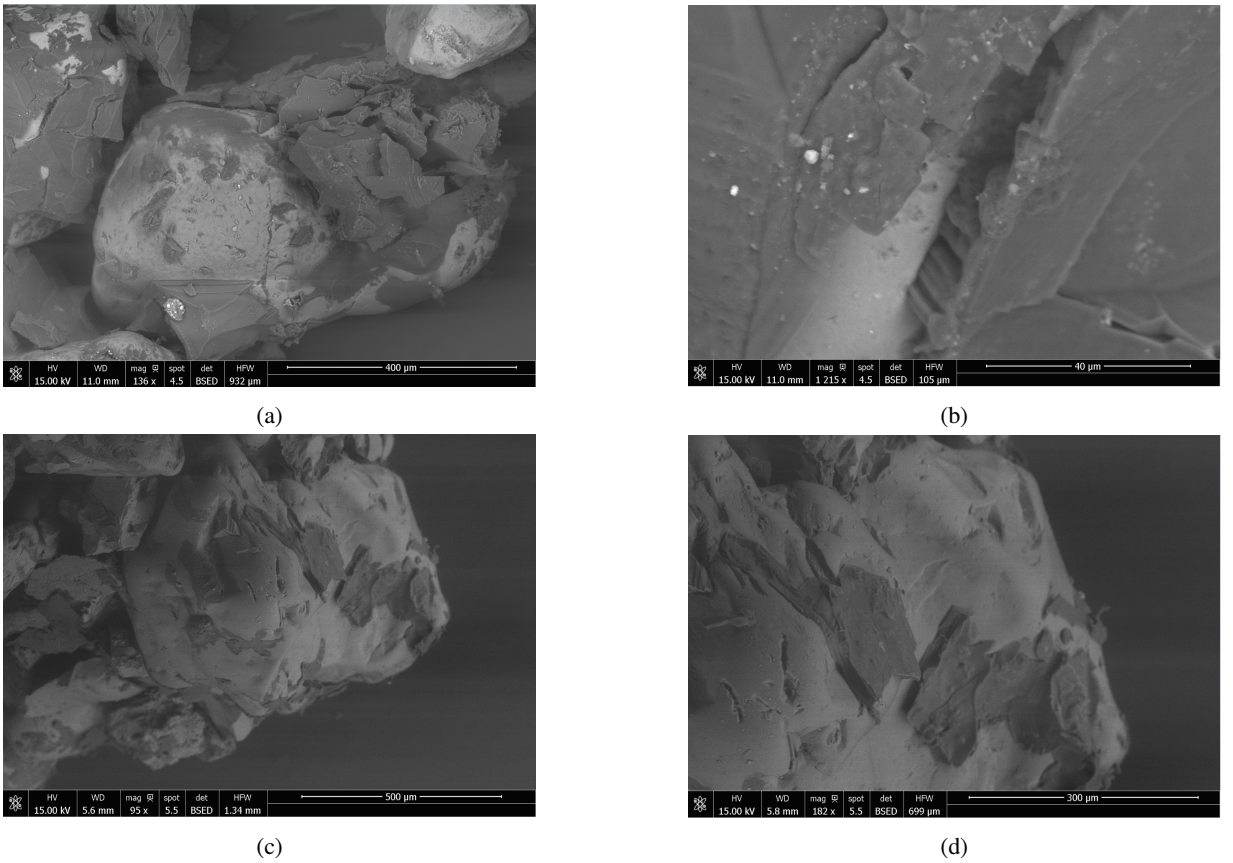

Figure 9: SEM images of sugar-cemented sand at various magnifications from SC20-CT105-T5: (a) overview at 136× magnification showing a sand grain (light grey) with sugar deposits (dark grey) attached along its surface; the sugar exhibits sharp edges indicative of crystalline formation; (b) Detail at 1215× magnification highlighting the intimate contact and bonding between the sugar and sand particles; (c) lower magnification image (95×) illustrating a sand grain with visible sugar accumulations; (d) magnified view of the sugar matrix in (c), where the angular morphology of the sugar crystals is evident.

7. Conclusions

This study demonstrates that ordinary household sugar can act as a rapid, effective, and biodegradable cementing agent for dry sand. Unconfined Compressive Strength (UCS) values ranged from approximately 1 MPa to over 6 MPa, depending on sugar concentration and curing conditions, with optimal performance achieved under moderate oven-drying at 105 °C for 24 hours.

From a macro-mechanical perspective, UCS stress–strain responses were characterised by a near-linear stiffness up to peak stress, followed by softening. Stress-strain response were characterised by: nearly a linear response till peak (with secant stiffness affected primarily by curing), a peak resistance associated with tensile cracking (affected by both curing and sugar content), and a softening rate (mostly influenced by sugar content rather than curing protocol). Findings include the following mechanical characterisation:

- UCS increased with sugar concentration from about 1.5 MPa at 15% sugar to over 6 MPa at 40% sugar when cured at ideal curing conditions of 105 °C for 24 h. For alternative curing conditions (60 °C for four days or 170 °C for five hours) consistently yielded mean strengths above 1 MPa. Notably, the UCS data showed low variability (coefficient of variation <16%) across specimens prepared under identical conditions.

- Secant stiffness at peak stress reached approximately 350 MPa under ideal curing and high sugar concentration, on par with or exceeding values reported for more complex bio-cementation techniques. Lower curing temperatures (60 °C) and high-temperature exposure (170 °C) yielded average stiffness values around 150 MPa. In

contrast to UCS, stiffness exhibited significant variability (up to 60%), limiting its reliability as a standalone design parameter.

- Curing at 105 °C for 24 h provided the best balance between rapid hardening and strength development. Lower temperatures required longer drying periods to achieve moderate strength (1.3 MPa at 60 °C), while excessive heating at 170 °C induced sugar caramelisation, reducing strength to 1.2 MPa.

In terms of the microstructure of the sugar-crystal to sand particle aggregates, scanning Electron Microscopy (SEM) confirmed extensive sugar crystallisation at intergranular contacts, forming angular, interlocking bridges that transmit tensile loads. This microstructure explains the consistent axial splitting observed in post-test specimens and supports the interpretation of sugar cementation as a tension-dominated failure mechanism.

Compared to established methods—such as Microbial-Induced Calcite Precipitation (1.5 MPa to 5 MPa), fungal biocementation (1 MPa to 4 MPa), or xanthan gum treatments (0.3 MPa to 4 MPa), sugar-cemented sand offers competitive UCS performance. It also provides distinct practical advantages: the sugar solutions used are non-toxic, exhibit low viscosity (e.g., 1.2 mPa s at 20% sugar), and preserve the native porosity and permeability of the sand matrix. Furthermore, sugar cementation is both reversible and biodegradable. Upon rewetting, the sugar bonds dissolve, enabling controlled disaggregation—an important feature for temporary stabilisation applications such as emergency airstrips, erosion control, or laboratory-scale physical modelling.

Future research should focus on hybrid strategies that combine the immediate mechanical benefits of sugar-induced hardening with the longer-term effects of fungal bio-cementation. In particular, efforts are needed to evaluate the durability and moisture sensitivity of sugar-cemented sand under realistic field conditions, quantify the degradation and reactivation potential of sugar bonds upon wetting and drying cycles, and develop constitutive models that capture the dependence of mechanical behaviour—such as stiffness, strength, and softening—on sugar concentration and curing parameters. By establishing the scientific basis of this simple and reversible physical cementation mechanism, the study opens new directions for low-impact, biodegradable ground improvement strategies in sustainable geotechnical engineering.

Nomenclature

C_f	Curvature coefficient [-]
D	Diameter of the sample [m]
ε_{UCS}	Axial strain at UCS [-]
e	Void ratio [-]
$E_{\text{sec,50}}$	Secant modulus at 50% of UCS [MPa]
$E_{\text{sec,UCS}}$	Secant modulus at UCS [MPa]
H	Height of the sample [m]
U	Uniformity coefficient [-]
UCS	Peak unconfined compressive strength [MPa]

8. Acknowledgements

GS and IR acknowledge that this work is part of the Soil Is Alive (SoIA) project, funded by the Carlsberg Foundation under the Semper Ardens: Accelerate Consolidator Excellence Grant.

CRediT authorship contribution statement

Gianmario Sorrentino: Conceptualization, Data curation, Formal analysis, Investigation, Methodology, Validation, Visualization, Writing – original draft. **Andrea Franza:** Methodology, Formal analysis, Visualization, Writing – review & editing. **Irene Rocchi:** Funding acquisition, Writing – review & editing.

References

Abbasi, F., Choobbasti, A. J., and Roushan, K. (2025). Advanced stabilization of clayey sand using xanthan gum: insights from multiscale evaluation and ultrasonic pulse velocity analysis. *Results in Engineering*, 25:104419.

Abdelhak, M. (2022). Soil improvement in arid and semiarid regions for sustainable development. In *Natural resources conservation and advances for sustainability*, pages 73–90. Elsevier.

Ahmad, J., Khan, M. A., Ahmad, S., Alkahtani, M. Q., Mursaleen, M., and Islam, S. (2024). Visualising the strength development of ficp-treated sand using impedance spectroscopy. *Scientific Reports*, 14(1):24115.

ASTM (2010). Standard test method for unconfined compressive strength of cohesive soil.

ASTM (2017). Astm d2487-17e1: Standard practice for classification of soils for engineering purposes (unified soil classification system). Astm.

Atkins, P. W., Jones, L., and Laverman, L. (2005). *Principi di chimica*. Zanichelli.

Chen, Y. and Yang, J. (2023). Small-strain shear modulus of silty sands: the role of sample preparation method. *Géotechnique*, 74(4):367–382.

Collins, B. D. and Sitar, N. (2009). Geotechnical properties of cemented sands in steep slopes. *Journal of geotechnical and geoenvironmental engineering*, 135(10):1359–1366.

Das, B. M. (2019). *Advanced soil mechanics*. CRC press.

de Bono, J., McDowell, G., and Wanatowski, D. (2015). Investigating the micro mechanics of cemented sand using dem. *International Journal for Numerical and Analytical Methods in Geomechanics*, 39(6):655–675.

Ding, H., Yang, Z. A., and Geng, X. (2023). A study on the durability of xanthan gum strengthened sandy loam.

Edinçliler, A., Baykal, G., and Saygılı, A. (2010). Influence of different processing techniques on the mechanical properties of used tires in embankment construction. *Waste Management*, 30(6):1073–1080.

Fang, C., Kumari, D., Zhu, X., and Achal, V. (2018). Role of fungal-mediated mineralization in biocementation of sand and its improved compressive strength. *International Biodeterioration & Biodegradation*, 133:216–220.

Gomez, M. G., Anderson, C. M., DeJong, J. T., Nelson, D. C., and Lau, X. H. (2014). Stimulating in situ soil bacteria for bio-cementation of sands. In *Geo-congress 2014: Geo-characterization and modeling for sustainability*, pages 1674–1682.

Haeri, S., Noorzad, R., and Oskoorouchi, A. (2000). Effect of geotextile reinforcement on the mechanical behavior of sand. *Geotextiles and Geomembranes*, 18(6):385–402.

Huang, J. and Hartemink, A. E. (2020). Soil and environmental issues in sandy soils. *Earth-Science Reviews*, 208:103295.

Imani, S., Soltani-Jigheh, H., Kafil, H. S., Zinatloo-Ajabshir, S., and Fahmi, A. (2025). Environmental sustainability in combating wind erosion: Chemical stabilization of sand dunes using acidic mulching. *Results in Engineering*, 25:103758.

Izadi, R., Allahverdi, A., et al. (2022). An overview of methods and materials for sandy soil stabilization: emerging advances and current applications. *ECOPERSIA*, 10(4):333–347.

Jefferis, S. (2003). Grouts and grouting. *Advanced Concrete Technology Set, Elsevier, Oxford*.

Jiang, N.-J. and Soga, K. (2017). The applicability of microbially induced calcite precipitation (micp) for internal erosion control in gravel–sand mixtures. *Géotechnique*, 67(1):42–55.

Jin, Z., Wang, G., George, T. S., and Zhang, L. (2024). Potential role of sugars in the hyphosphere of arbuscular mycorrhizal fungi to enhance organic phosphorus mobilization. *Journal of Fungi*, 10(3):226.

Kazemian, S., Huat, B. B., Arun Prasad, A. P., and Barghchi, M. (2010). A review of stabilization of soft soils by injection of chemical grouting.

Khatami, H. R. and O'Kelly, B. C. (2013). Improving mechanical properties of sand using biopolymers. *Journal of Geotechnical and Geoenvironmental Engineering*, 139(8):1402–1406.

Kim, E. (2010). Relationship between viscosity and sugar concentration in aqueous sugar solution using the stokes' law and newton's first law of motion.

Konstantinou, C., Wang, Y., Biscontin, G., and Soga, K. (2021). The role of bacterial urease activity on the uniformity of carbonate precipitation profiles of bio-treated coarse sand specimens. *Scientific reports*, 11(1):6161.

Kosmas, C., Tsara, M., Moustakas, N., Kosma, D., and Yassoglou, N. (2006). Environmentally sensitive areas and indicators of desertification. In *Desertification in the Mediterranean region. A security issue*, pages 525–547. Springer.

Leaper, M. C., Berry, R., Bradley, M., Bridle, I., Reed, A., Abou-Chakra, H., and Tüzün, U. (2003). Measuring the tensile strength of caked sugar produced from humidity cycling. *Proceedings of the Institution of Mechanical Engineers, Part E: Journal of Process Mechanical Engineering*, 217(1):41–47.

Lee, J., Roux, S., Le Roux, E., Keller, S., Rega, B., and Bonazzi, C. (2022). Unravelling caramelization and maillard reactions in glucose and glucose+ leucine model cakes: Formation and degradation kinetics of precursors, α-dicarbonyl intermediates and furanic compounds during baking. *Food Chemistry*, 376:131917.

Makusa, G. P. (2012). Soil stabilization methods and materials. *Lulea University of Technology*.

Martuscelli, C., Soares, C., Lima, N., and Camões, A. (2020). Potential of fungi to produce biosandstone. *RILEM Technical Letters*, 5:157–162.

Meadows, D. (1993). Somewhat dry... a new look at the conditioning of refined sugar. *Proceedings of The South African Sugar Technologists' Association, Durban, South Africa*.

Mitchell, J. K. and Soga, K. (2005). Fundamentals of soil behavior 3rd ed., johnwiley &sons. *Inc. Foundation failure*.

Mould, J.C., J. (1983). *Stress Induced Anisotropy and the Evaluation of Multi-surface Elasto-plastic Material Model*. PhD thesis.

Nemati, N. (1986). Pasture improvement and management in arid zones of iran. *Journal of arid environments*, 11(1):27–35.

Park, J. S., Lin, H., Chen, E., Alqrinawi, H., Dong, Y., and Moe, W. M. (2025). Mechanical properties of fine-grained soils treated with fungal mycelium of trichoderma virens. *Journal of Geotechnical and Geoenvironmental Engineering*, 151(5):04025030.

Pérez, S. (1995). The structure of sucrose in the crystal and in solution. In *Sucrose: Properties and Applications*, pages 11–32. Springer.

Petersen, N. B., Bastola, A., Akula, P., and Rushing, J. (2025). Physicochemical kinetics of rapid soil stabilization using calcium sulfoaluminate-based cements. *CEMENT*, page 100134.

Prabakar, J., Dendorkar, N., and Morchhale, R. (2004). Influence of fly ash on strength behavior of typical soils. *Construction and Building Materials*, 18(4):263–267.

Rafalko, S. D. (2006). *Rapid soil stabilization of soft clay soils for contingency airfields*. PhD thesis, Virginia Tech.

Rahman, M. M., Hora, R. N., Ahenkorah, I., Beecham, S., Karim, M. R., and Iqbal, A. (2020). State-of-the-art review of microbial-induced calcite precipitation and its sustainability in engineering applications. *Sustainability*, 12(15):6281.

Ryer-Powder, J. E. (1991). Health effects of ammonia. *Plant/operations progress*, 10(4):228–232.

Schmidt, S. J., Thomas, L. C., and Lee, J. W. (2012). Response to comment on the melting and decomposition of sugars. *Journal of agricultural and food chemistry*, 60(41):10363–10371.

Soldo, A. and Miletić, M. (2019). Study on shear strength of xanthan gum-amended soil. *Sustainability*, 11(21):6142.

Sorrentino, G. (2022). *Effects of filtration process variables on filter cake properties and formation*. PhD thesis.

Sture, S., Alqasabi, A., and Ayari, M. (1999). Fracture and size effect characters of cemented sand. *International journal of fracture*, 95:405–433.

Tariq, K. and Maki, T. (2014). Mechanical behaviour of cement-treated sand. *Construction and Building Materials*, 58:54–63.

Tester, C. F. (1990). Organic amendment effects on physical and chemical properties of a sandy soil. *Soil Science Society of America Journal*, 54(3):827–831.

Zhang, X., Li, Z., Tai, P., Zeng, Q., and Bai, Q. (2022). Numerical investigation of triaxial shear behaviors of cemented sands with different sampling conditions using discrete element method. *Materials*, 15(9):3337.

Zhelezova, A., Sorrentino, G., Otim, G. I., and Rocchi, I. (2025). Soil is alive–how does soil biota influence soil mechanical properties? a perspective review. *Biogeotechnics*, page 100175.

Zhu, J., Wei, R., Peng, J., and Dai, D. (2024). Improvement schemes for bacteria in micp: A review. *Materials*, 17(22):5420.

Supplemental Materials

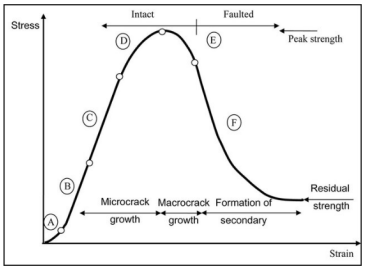

Figure S1: A description of rock deformation.